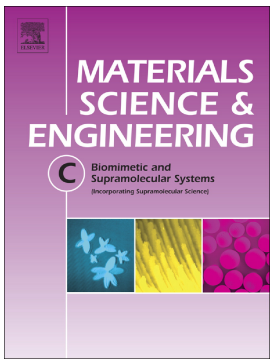

A novel approach to enhance the spinnability of collagen fibers by graft polymerization

Zahra Bazrafshan, George K. Stylios

PII: S0928-4931(17)34505-8
DOI: doi:10.1016/j.msec.2018.09.016
Reference: MSC 8879

To appear in: *Materials Science & Engineering C*

Received date: 16 November 2017
Revised date: 23 August 2018
Accepted date: 6 September 2018

Please cite this article as: Zahra Bazrafshan, George K. Stylios , A novel approach to enhance the spinnability of collagen fibers by graft polymerization. Msc (2018), doi:10.1016/j.msec.2018.09.016

A novel approach to enhance the spinnability of collagen fibers by graft polymerization

Bazrafshan Zahra, Stylios George K.

Research Institute for flexible materials, Heriot-Watt University, UK
Corresponding Author: Zahra Bazrafshan (E-mail: zb4@hw.ac.uk)

ABSTRACT

Collagen is an important natural biopolymer that cannot be electrospun easily due to the lost properties occurs in the associated degrading chains while dissolving and spinning. Grafting polymerization of methyl methacrylate-co-Ethyl Acrylate was applied to modify the surface of acid soluble collagen (ASC). The branched copolymer on the surface of collagen significantly influenced the initial viscosity. Since chain entanglement is crucial for fiber formation during electrospinning, the dependency of entanglement concentration on branch densities possessing the approximate same viscosity was investigated; in which the mean fiber diameters of all considered samples remained broadly constant. Increasing the number of branching onto ASC chains significantly decreased the deteriorative impact of the electrospinning conditions. It has also increased the stability of the collagen-based fibers under high humidity conditions. The short chain branched ASC-g-P(MMA-co-EA) can effectively influence the thermal stability of electrospun collagen fibers while the long chain branched ASC-g-P(MMA-co-EA) can provide a higher chain entanglement density leading to the more fiber uniformity.

KEYWORDS: Collagen, Graft polymerization, Electrospinning, Chain entanglement, Thermal behavior, Surface Wettability, Water absorption

1- Introduction

Development of newly engineered materials with desired properties e.g. thermal, mechanical or biological for specific applications is an important field in material sciences [1-3]. In biomaterial and particularly in natural-based polymers, it is essential to modify their properties to desired conditions for specific end uses [4, 5].
Collagen and its associated derivations are the leading natural biomaterials with excellent biological and physiochemical properties that have been used in a variety of applications such as in drug delivery [4, 6], filtration [7, 8], tissue scaffolds [9, 10], protective clothing [11], wound dressing [12]. Attempts have been made to modify collagen by graft polymerization to benefit from its natural properties whilst at the same time, to add value by introducing monomer(s) to its main chain [13, 14].
Thus far, the main objective of many research groups has been focused on reducing the highly hydrophilic behavior of collagen chains and benefiting in a controllable degradation by using the graft polymerization method [13, 15-18]. This method is well known for producing collagen-based hydrogels [15, 19-22].
When it comes to promoting the final product with a high surface area, the electrospinning technique is an attractive method for the processing of polymeric fibers with a wide range of diameters from a few microns down to 100 nm. In general, the electrospun fibers can be achieved by altering the processing and polymer melt/solution parameters [23, 24].
However, Zeugolis et al. reported that physiochemical properties of the pure collagen are lost when it is electrospun into fibers [25]. They observed a lowered denaturation temperature in electrospun collagen chains that was also confirmed by some recently published studies [26, 27]. In a similar work, Yang et al. revealed that 45% of the collagen mass is denatured during electro-spinning [28]. Furthermore, due to a significant conformational change in collagen chains, it has been reported that the electrospun collagen fibers do not swell in aqueous media and may immediately dissolve in water [9, 28-31].
To reduce the negative effect of processing methods on sensitive structure of collagen chains, surface

modification methods on collagen fibers using crosslinking agents have been extensively recommended as post-treatment [23, 24, 32, 33]. For instance, chemical crosslinking agents such as aldehydes have been typically applied to protect the collagen fibers obtained from electrospinning [23, 24]. However, due to random crosslinking, the end material is more likely to lose its desired morphology after post- treatment [34]. Also, the rigid and fixed collagen chains are incapable to represent good mechanical properties rendering the material to suffer under non-stable humidity conditions [23].

To the best of our knowledge, the effect of flexible branching chains onto the structure of collagen has not been given attention when the grafted polymer is electrospun into fibers. We hypothesize that during the electrospinning process, the branching on the main backbone of collagen can significantly preserve the collagen from an extensive conformation change by the electrostatic repulsion force occurring between its chains in acidic solvents. And branch densities can present different velocities by influencing chain entanglement which is essential in fiber formation.

In this study, Collagen was solubilized by acid treatment. Subsequently, binary different vinyl monomers of Methyl Methacrylate (MMA) and Ethyl Acrylate (EA) in varied feed ratios were grafted onto the acid soluble collagen (ASC) to achieve collagen graft polymers with varied branch densities. To exploit the advantages of the chain flexibility of the structurally branched copolymer, the collagen graft copolymers were then processed through the electrospinning method in low concentrations. The effect of entanglement density on fiber diameters was investigated. Our aim is to benefit from the amphiphilic behavior, the firmness and the plasticizing capacity of the resulted copolymer under unstable humidity conditions. Since electrospinning is believed to be a challenging processing method for the sensitive nature of collagen chains, we performed surface characterizations on the electrospun fibers from the collagen graft copolymers. To investigate the degradation and water absorption capacity of the collagen-based fibers, a series of comparisons were performed between the unprocessed bulky graft collagen copolymers and the fibers. This controlled branching can be used as a predictable method to preserve the morphology of the collagen-based fibers, in contrast with randomly crosslinking methods which pose significant challenges.

2- Materials and methods

2.1. Materials

Collagen from cow skin was provided by Devro Company Inc., UK. Methyl methacrylate (MMA, 99%, Alfa Aesar), Ethyl Acrylate (EA, 99%, Alfa Aesar) were used as monomers and were passed through a column of 5% sodium hydroxide acquis solution to remove inhibitors existing in the monomers. Benzoyl peroxide (BPO, 97%, Alfa Aesar) was used as initiator and recrystallized in Acetone before applying. Acetic acid (AA, 99.7%, Alfa Aesar), Formic Acid (FA, 99%, Alfa Aesar), distilled water and methanol (MeOH, 99.9%, Alfa Aesar) were applied as received.

2.2. Graft polymerization onto Acid Soluble Collagen (ASC)

ASC was prepared using pure collagen from cow skin in 100 mmol AA and distilled water (Table 1) to reach to pH of 3±1. The mixture was incubated for 5 h at 45 °C in a 250-ml triple necked round-bottom flask and a stirrer bar was then added. This step was terminated by the suddenly increased temperature of 80°C, the threshold of achieving ASC in water, seen as a homogenous solution.

Free radical polymerization was used to synthesize the graft copolymers of MMA and EA onto ASC in distilled water. This procedure is given in detail elsewhere [35, 36]. In this step, the previous 250-ml triple necked round bottomed flask was served as a reaction vessel. Nitrogen gas was applied through the solution while stirring. Once the desired temperature (80 °C) was achieved, dissolved BPO in 2 ml Acetone as the initiator, was added gradually to the reaction vessel within 10 min. Distilled MMA and EA in the rates mentioned in Table 1, were then introduced to the mixture via a syringe in 30 min. The temperature and reaction time were fixed at 80°C and 60 min after adding the initiator and the monomers. The stirrer speed was also fixed at 2400 rpm during the reaction. Precipitation of the graft copolymer occurred after 15 min of reaction time yielding a milky white solution. The reaction mixture was then added to excess cool methanol for complete precipitations. The solution was then filtered with a glass sinter filter and dried in a vacuum oven at 25 °C until a constant weight was achieved. Accordingly, 5 samples (S1P2… S5P2) were obtained as listed in Table 1.

As with any conventional free radical copolymerization reaction, the formation of P(MMA-co-EA) always arises along with that of the desired copolymer (ASC-g-P(MMA-co-EA) due to reactivity ratio effects or the segregation of macromonomers from main and side chains. An extraction step was required to remove

ungrafted ASC, unreacted EA and MMA macromonomer and P(MMA-co-EA) from the collagen graft copolymers.

Table 1 Change of graft performance with water content and initiator concentration based upon the feed ratio composition for reactants used in the synthesis of grafted copolymers (initial amount of ASC was set at 11g)

Sample	Comonomer cont. in feed (mmol)	EA cont. (%)	Feed ratio ASC:(MMA-co-EA) (wt.: wt.)	Water cont. (mL)	Initiator (mmol)	GP (%)	GE (%)	Yield of grafted collagen (%)	$Mn*10^{-3}$ of Branch copolymer	Wight ratio of ASC: Side grafts	Nitrogen cont. %
S1P2	109.83	0.50	1:1	85	4.51	11.42	10.79	6.26	9.54	1:0.96	7.46
S2P2	219.71	5.00	1:2	106	9.10	37.14	16.47	21.85	7.89	1:1.09	4.69
S3P2	329.65	10.00	1:3	120	13.62	49.85	15.68	32.47	7.08	1:1.33	4.59
S4P2	493.47	15.00	1:4	145	18.16	57.42	13.49	34.37	8.06	1:1.68	4.35
S5P2	549.39	20.00	1:5	160	22.70	51.71	10.34	32.13	9.11	1:1.53	5.95

A simple isolation method with selective solvent extraction based upon the difference in the solubility was employed. Therefore, the grafted copolymers were extracted by repeated washings with hot water followed by acetone at room temperature to remove the associated ungrafted ASC and P(MMA-co-EA). The supernatants were then separated from the graft copolymer using a sintered glass filter under reduced pressure. All samples were dried in a vacuum oven at room temperature until constant weight was achieved. The grafting percentage (GP) and the grafting efficiency (GE) were calculated by the following equations:

$$GP = \frac{W1 - W0}{W0} \qquad (1)$$

$$GE = \frac{W1 - W0}{W2} \qquad (2)$$

Where W_0, W_1, and W_2 are the weights of the initial ASC and ASC-g-P(MMA-co-EA) and the used comonomers, respectively [36, 37].

To calculate the Yield of the graft collagen, the collagen graft copolymer was hydrolyzed in HCl and the weight of branch copolymer was evidence to measure the Yield of the graft collagen using the given equation:

$$\text{Yield of the graft collagen} = \frac{(W1 - W2) - W0}{W0} \qquad (3)$$

Where W_0, W_1, and W_2 were the weights of the initial ASC, ASC-g-P(MMA-co-EA), and the grown branches, respectively [38]. The molecular weight of the isolated grafted branches was then determined by viscometric measurements in Acetone at 30°C, based on the relation $(\eta) = 7.70\times10^{-3}M_n^{0.70}$.[38]

2.3. Preparation of the electrospinning solution, fiber formation, and characterizations

The above-obtained collagen graft copolymers were then dissolved individually in FA and stirred at room temperature until homogenous solutions were achieved. To investigate the effect of P(MMA-co-EA) content, each solution was then transferred into the 5-ml plastic syringe connected to a needle (22-gauge) to be processed. A Spreybase® electrospinning system was used to process all solutions at the following conditions: feed-rate (1 ml min^{-1}), needle diameter (gauge 22), temperature (25±2°C) and humidity (RH: 35-40%) (using IR lamp), TCD (15 cm, distance between the tip of needle and the fiber collector), voltage (10 kV) and different solution concentrations with approximately same viscosity. A grounded rotating collector (surface length of 25 cm, diameter of 9 cm) at a speed of 1.7 ms^{-1} was used.

To measure the Nitrogen content of the collagen graft copolymers, an Exeter CE-440 Elemental Analyzer was used. The conductivity value of the sample solutions was determined using a conductivity meter (OAKTON, RS232 CON 110 series). Surface tension studies of the solutions were carried out by using a tensiometer (KRŰSS). Inherent viscosities of diluted polymer solutions (1 wt%) in FA were determined using a Brookfield DV-II+Pro Viscometer at (20 ± 0.2) °C. The structure of the electrospun fibers was revealed by Fourier Transform Infrared Spectroscopy (FT-IR, Thermo Nicolet Avatar 370 DTGS) at room temperature after washing the fibers with warm distilled water (40℃). To prepare the disk, fibers (1 wt%) in KBr were uses. High-resolution ^{1}H-NMR spectra were recorded on a Buker AVI-400 spectrometer. To compare signals of the end groups before and after electrospinning, the processed and unprocessed collagen graft copolymers were dissolved in deuterated acetic acid.

The structure of the fiber samples was also characterized by X-ray diffraction (XRD) using a Bruker D8 Advance powder diffractometer. The X-ray diffraction patterns were collected from 5° to 60° in 2θ value (wavelength of 1.5406 Å) over one hour per sample using Ge-monochromated Cu Kα radiation and zero background sample holder. The

generator settings were at 40kV, 40mA and the sample was rotated at 30 rpm.

The morphology of the fibers was studied using Scanning Electron Microscopy (SEM, Hitachi S-4300). The mean fiber diameter and uniformity of the fibers were estimated statistically by using ImageJ software from SEM micrographs. The thermal analysis of the achieved fibers was performed by Differential Scanning Calorimeter (DSC, Mettler DSC 12E). A temperature ranging up to 220 °C with a heating rate of 10 °C min^{-1} in the nitrogen atmosphere was reached. Sensitivity curve analysis was carried out on samples (10 mg) to evaluate changes in their thermal behavior. Thermogravimetric analysis (TGA) was carried out by using a thermogravimetric analyzer (Mettler TC 10A/TC 15 Instrument) range of 35– 600°C on samples (5 mg) at a heating rate of 10 °C min^{-1}. The water contact angles of different fiber samples were measured by a contact angle analyzer (OneAttention v. 2.3, Boilin Scientific, n=5). Heat and mass transfer mechanisms were studied by weighing the fiber samples (n=5) before and after immersion in distilled water. Excess water was removed from the samples by gently blotting with filter paper prior to each weighing.

3- Results and Discussions

The solubility profile of ASC and the graft polymerization process were presented by four controlled parameters including; temperature, rotation speed, and time (Figure 1, supplementary information). Table1 gives a summary of the amount of raw material used in the current study. In all experiments, 11g ASC was used and various MMA-co-EA feed ratios were examined. The incorporation of the growing branches onto ASC chains correlates well with the feed ratios of MMA-co-EA in the reaction. More specifically, the grafting performance and the yield of grafted collagen confirm the direct interaction of the feed ratio of co-monomers added to ASC chains. This can be due to the steric effect and polarity effect of the combination of ASC and co-monomers in the aqueous medium.

According to Table 1, a decrease in the grafting performance is evident at the highest feed ratio of S5P2 where the dominated co-monomers are more likely to be initiated and to be (co)polymerized solely in the reaction. Furthermore, S2P2, S3P5 and S4P2 represent a decreased molecular weight of branch copolymers, higher grafting efficiencies, and lower Nitrogen contents in contrast with other samples. This may be due to increased number of grafting points on the ASC backbone.

As shown in Table 2, the conductivity of the dissolved copolymers having dielectric properties was studied to compare the effect of P(MMA-co-EA) content on the charge dynamics of chains. The cationic characteristic of ASC is responsible for the higher electric conductivity compared to the P(MMA-co-EA) with low dielectric constant when they are bonded covalently on the surface of collagen chains [39]. ASC-g-P(MMA-co-EA) showed a reducing electron mobile phase with increasing the branch densities on ASC. The replacement of Hydrogen compounds on ASC to MMA-co-EA can lead to dropping conductivity of the solutions. Hence, the conductivity value of S1P2 and S5P2 can be due to having the lowest number of side branches on the backbone of ASC (Table 2).

Table 2 Properties of the electrospinning solutions

Sample	Concentration (% wt./v)	Viscosity (cP)	Conductivity ($ms.cm^{-1}$)	Surface tension ($mN.m^2$)
S1P2	10.17	120±10	3.23	31
S2P2	6.07	120±10	1.02	30.5
S3P2	6.97	120±10	1.01	33
S4P2	4.14	120±10	1.02	31.5
S5P2	5.48	120±10	2.91	33

With the knowledge that the surface tension of polymeric solutions tends to increase with the growth of M_n, the interfacial phenomena of the prepared solutions were evaluated by applying the Nouy ring method. Although the corresponding values in Table 2 show a slight increase to some extent in some samples, all surface tension values are in the range of 31.8±1.02. This is possibly due to the wide molecular weight distribution occurred in ASC extraction as well as the side branching growth on the main backbone of ASC.

Generally, the fact that chain entanglements making concentration, and consequently viscosity are essential for fiber formation, has been well established [32, 40] and it has also been repeatedly reported that the diameter of electrospun fibers can be increased by increasing solution viscosity [31, 41-43]. By contrast to the widely-studied electrospinning of homopolymers, the electrospinning of branched copolymers has an additional less known aspect; namely the chain entanglement density as one of the many parameters affecting the fiber formation and surface morphology. While in electrospinning, the importance of chain entanglements has been widely accepted, there is no clear understanding on the required entanglements to stabilize the fiber formation of non-linear polymers. This issue becomes more crucial when one segment of

copolymers; in this case ASC, is more likely to be non-stable during electrospinning [9, 28-31, 44].

Hence, the chain entanglement concentration (C_e) was assumed to be dependent on the density of branching on ASC along with solvent power in which FA was used as a suitable solvent for both segments of branches and main chain in all studied samples. We applied a range of comonomer feed ratios to study the effect of increased side branches on the collagen chain against repulsive forces during electrospinning which caused by factors such as solvent power and high intensity of electric field. Also, the effect of branching on chain entanglement density of samples was considered through fiber formation of various sample solution concentrations representing approximately a same viscosity while all other factors were constant.

As shown in Figure 1, the surface morphology of all electrospun samples looks similar at first glance, without bead deficiencies, suggesting the polymer concentrations shown in Table 2 are above $2C_e$, where C_e is a function of chain density and intermolecular interactions [45].

Based on the above-given arguments, it is important to consider the concentration dependence of the diluted solutions of 1 w/v % ASC-g-P(MMA-co-EA) in FA. The changed density of branching displayed significantly different viscosities (η).

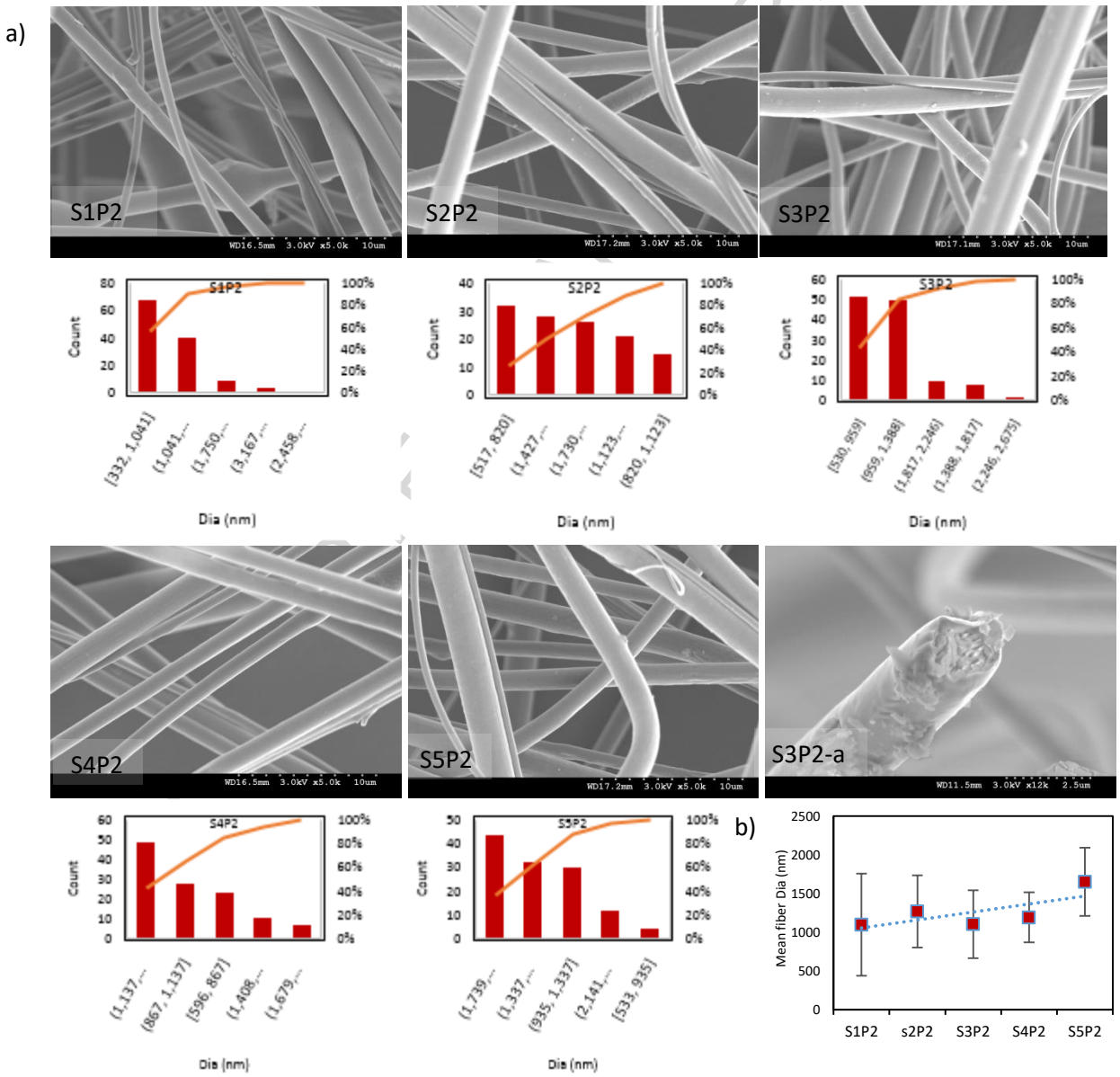

Figure 1 a) SEM micrographs and associated fiber diameter scattering of grafted polymer S1P2 …S5P2 and a representative capture of a cross-sectional SEM image of S3P2 formed with feed-rate (1 ml min^{-1}), needle diameter (gauge 22), temperature (25±2^{o}C) and humidity (RH: 35-40%), TCD (15 cm), and voltage (10 kV), b) The effect of P(MMA-CO-EA) content on mean fiber diameter and uniformity (standard deviations) of the fibers.

Fig. 2 shows that over the shear rate range investigated, the grafted copolymer displayed Newtonian behavior. With the knowledge of having a higher absolute Mw, the highly-branched copolymers can display a higher viscosity compared to lower degrees of branching obtained in S1P2 with the possessing of lowest comonomer feed ratio.

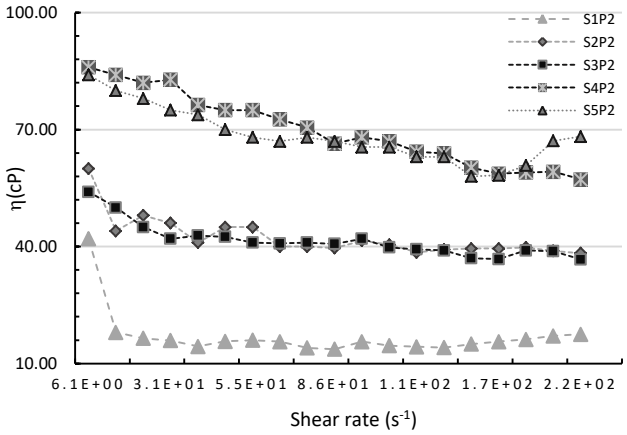

Figure 2 Shear rate dependence of viscosity for different co-monomer feed ratio. All copolymers showed Newtonian behaviour over the range of shear rates studied.

Fig. 1 exhibits the SEM micrographs and the associated fiber diameter scattering of grafted copolymer S1P2 to S5P2 and also a typical example of the cross-sectional SEM micrograph of S3P5 (S3-a) in which the phase separation behavior of the electrospun copolymer is observed through the porous fibers.

Fiber diameter scattering of each sample was also demonstrated in the associated Pareto graph in which the individual scattering values of each specific fiber diameter range is denoted in downward order by bars, and the cumulative total is indicated by the line (Fig. 1a). The highest frequency distribution of S1P2 was in the range of (332-1041 nm) while S2P2 to S5P2 possess their frequency distribution to a greater extent of fiber diameter in the following order: (S2P2, 517-820 nm), (S3P2, 530-959 nm), (S4P2, 1137-1408 nm), and (S5P2, 1739- 2141 nm).

Figure 1b shows the correlation between the mean fiber diameters and P(MMA-co-EA) content of each sample incorporated into the precursor fibrous material. It must be noted that the bars on the plot are the standard deviations of fiber diameters. The standard deviations represent the uniformity of the electrospun fibers. Hence, S4P2 has the highest fiber uniformity whereas S3P2 represents the lowest average fiber diameter (1101 nm).

There is a clear correlation between the fiber diameters and the molecular weight of P(MMA-co-EA) contents in side chains influenced by monomer feed ratio, as discussed earlier, in which less average fiber diameter can be formed from collagen graft copolymers possessing the high density of short chains. These results are in good agreement with the viscosity graph, Figure 2 with a dramatic increase in the solution viscosity and the performance of highly branched polymers in fibrous assemblies which tells us the same story; that viscosity plays a leading role in fabrication of the fibers enabling chain entanglement during stretching of the solution jet towards the collector.

To verify our hypothesis, that the increased side chains can reduce the deteriorative effect of repulsive forces on collagen chains during the process, all electrospun samples were characterized by considering the FTIR and NMR spectra, XRD patterns, TGA and DSC plots. This is to get an insight into the electrospun ASC-g-P(MMA-co-EA) fibers which passed through the challenging process of electrospinning. And eventually, the functionality of the electrospun fibers was evaluated by additional measurements to determine their surface wettability and water absorption capacity.

The main characteristic features of the fiber samples were observed in the FTIR spectra, Figure 3. ASC has several characteristic absorption bands known as amide A (3425 cm^{-1}), amide B (2857-2953 cm^{-1}), amide I (1614-1711 cm^{-1}), amide II 1459 cm^{-1} in the infrared region of the spectrum [46, 47]. Characteristic bands of P(MMA-co-EA) were carbonyl (C=O) stretching vibration at 1730 cm^{-1}, CH (CH, CH_2 and CH_3) stretching vibrations at (2950-3050 cm^{-1}) (asymmetric) and (CH_2) 2865 cm^{-1} (symmetric), C-O stretching at 1060 cm^{-1}, and C-O-C stretching at 1260 cm^{-1} (asymmetric).

The amide I adsorption originated largely from the C=O stretching vibration and is specifically sensitive to the secondary structure of the polypeptides[48]. Hence, shift towards a higher wavenumber may represent hydrogen bonding formed between chains in S1P2 to S5P2.

The amide B and the amide II regions are affected by P(MMA-co-EA) absorptions. However, the amide A and amide I bands were used as reference peaks to confirm the presence of Collagen in the fibers of the graft copolymers in this analysis. Furthermore, two new

absorbance peaks can be observed in all samples; asymmetric vibration peak at 978 cm^{-1} referring to α to nitrogen linkage (N-C) and asymmetric stretching at 1158 cm^{-1} corresponding to (CO-O-C) that can be the branching points on the main backbone of ASC. In S3P2 and S4P2, a significant peak was observed at 1060 cm^{-1} associated with C-O-C stretching vibration and the highest intensity of C=O is observed in S4P2.

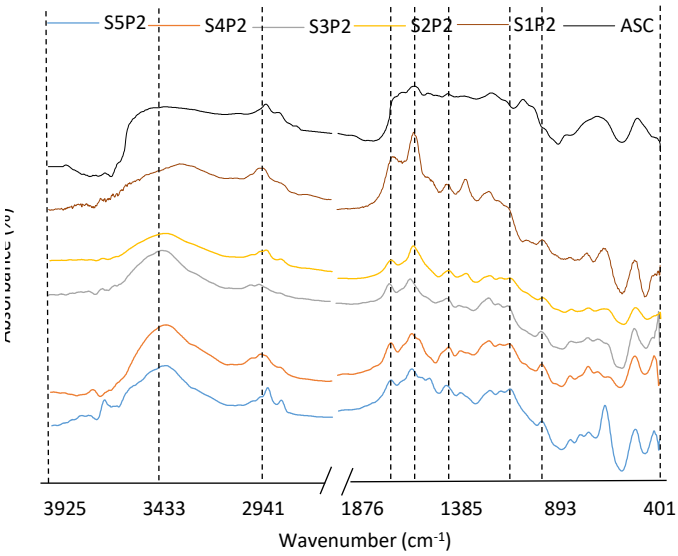

Figure 3 FTIR absorbance vs. frequency for Acid soluble collagen (ASC) and electrospun fiber samples with varied branching density of ASC-g-P(MMA-co-EA).

To further investigate into fiber compositions, TGA curves of the fiber samples of collagen graft copolymers was compared to the original ASC, as shown in Figure 4. TGA curves indicated that the dehydration (moisture loss) occurred in 50 to 200 °C [49] in all samples in the following order of mass loss: (ASC, %13.34), (S5P2, %10.23), (S1P2, S2P2 and S4P2, about %7.62), and (S3P5, %6.11).

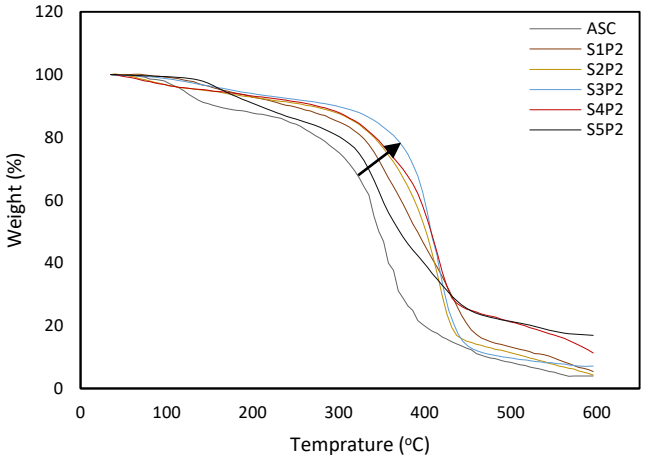

Figure 4 TGA analysis of the ASC and electrospun fibers from collagen graft copolymers of different comonomer feed ratio, S1P2…S5P2, heating rate of 10 °C.

The highest thermal stability was observed in the fiber sample of S3P5 at 380 °C while the other samples lost the same mass (about %24) at 307, 324, 346 and 360 °C for ASC, S5P2, S1P2 and (S1P2 and S4P2), respectively. The mass residuals at 550 °C were also significantly different; %5.75, %7.35, %9.32 and about 17% for ASC, (S3P2 and S2P2), S1P2 and (S5P2 and S4P2), respectively. This variation may be due to the carbonization of P(MMA-co-EA) that occurs in temperatures above 450 °C while the decomposition of ASC segment can be accomplished in temperatures below 450 °C [49, 50]. This reason can suggest that the analysis of TGA was accompanied by the carbonization of long side chains of methylene. Hence, the higher mass residual can confirm the presence of long grafted chains onto ASC backbone with the following order (high to low): S5P2, S4P2, S1P2, S2P2, S3P2, and ASC.

Furthermore, to analyze the chemistry of end-group variations before and after electrospinning, we characterized ^{1}H NMR spectra of the fiber samples and bulk collagen graft copolymers. This analysis was performed to study the end group signal changes that may be caused by processing factors. We assumed the changed signals in ^{1}H NMR spectra can represent chemical structure alterations caused by the denaturation of ASC during the process. Therefore, the less change in end group signals after the process in comparison with what recorded for the unprocessed copolymer can characterize more stability and processability of collagen graft copolymer as a key factor in the processing of biopolymers.

In ^{1}H NMR spectra, all samples of the bulk copolymers represent approximately the same main resonances in

varied intensities that can be attributed to protons of methyl (0.9-1 ppm), methylene (1.3-1.5 ppm), amine (-NH2, 1.35 ppm), R-N-C-R and R-CO-C-R (2-3 ppm, branching points), RO-CH_3 (3.64 PPM, side chains), and amide (R-CO-NHR, 7.5-8.5 PPM) as shown in Figure 5A.

The changes in signals of end groups of fiber samples are simply visible in Figure 5B in where S1P2 and S5P2 have received more structure alterations that were affected by the electrospinning parameters. More specifically, more changes occurred in the region of 1.35-5 ppm shifting to a higher electronegativity (deshielding). Furthermore, a significant increase in the integral value of amide signals from 7-9 ppm occurred, more specifically in S1P2, S2P2 and S5P2 after electrospinning that can be due to the amidation that caused by the electrospinning conditions, even though no clear sign of water existence was observed as a result of this reaction during the process. However, S3P2 and S4P2 underwent an insignificant structural change whereas S3P2 owning the highly short branch densities is the least affected collagen graft copolymer by electrospinning.

To better understand the branched structure of ASC, the graft copolymers and poly(MMA-co-EA), XRD spectra were considered, as shown in Figure 6. The broad peak of ASC at around $2\theta = 21.5^{o}$ is attributed to the overlapped diffraction from the collagen's crystal planes of (020) and (110), while the more intensive peak at $2\theta = 14.02°$ and also a weak peak at 29.68^{o} are observed in the Poly(MMA-co-EA)'s crystal planes of (110) and (200).

In the XRD spectra of graft copolymers, it can be observed that diffraction intensity of the peak at around 21.5° was obviously shifted to a lower angle, indicating that the crystallinity of the ASC decreased after grafting modification. Furthermore, P(MMA-co-EA) in S4P2 and S5P2 represent long enough chains that form a distinctive overlapped broad crystalline region at around $2\theta = 13°$.

The thermal behavior of the fiber samples from the graft copolymers was also investigated. As shown in Figure 7, the DSC curve of ASC demonstrates an endothermic peak at 85°C, 160°C and 220°C related to melting temperature (T_m) and denaturation process (T_d), respectively. In fiber samples, T_m dropped to a temperature between 59 to 80°C. This reduction in melting region can be affected by several parameters e.g. undergoing the slight denaturing of the backbone in the polymerization and subsequent electrospinning processes in which the average molecular weight may be lowered.

Also, as the thermal behavior is size dependent, this reduction can be explained by the size of the fiber samples in contrast with ASC, in the shape of the bulk polymer. The enthalpy of denaturation (ΔH_d), on the other hand, is not clearly observed in the fiber samples. This can be due to hidden peaks by transferring the samples into T_g of PMMA in the branches. These results indicate that ASC is thermally altered by the presence of side branched P(MMA-co-EA) in the feed ratios mentioned in Table 1, as verified by the shifting of the melting peak towards lower temperatures, with no

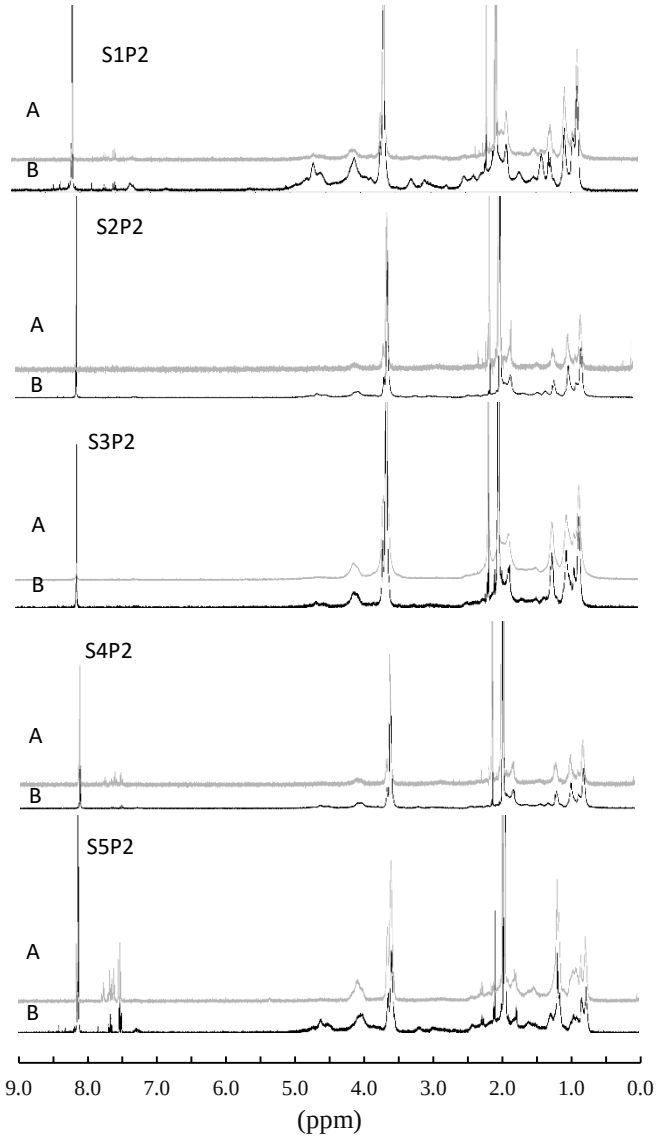

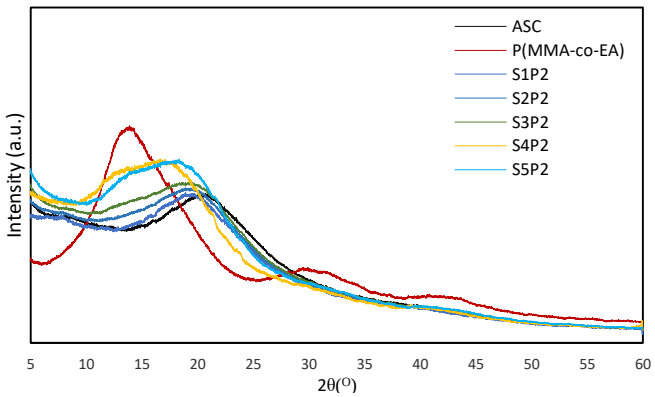

Figure 6 X-ray Diffraction (XRD) spectra of the electrospun fibers of collagen graft copolymers, ASC, and Poly (MMA-co-EA).

considerable changes on the enthalpy of denaturation, compared to non-processed ASC.

Overall, if we compare our results with those of Yang et al [28] in which they reported the melting point of 45 ^{o}C for pure collagen electrospun fibers, it can be realized that irrespective of the benefits of a tailored branching density, ASC modification by graft polymerization can improve the thermal stability of the electrospun fibers possessing a higher T_m of 59 to 71 ^{o}C.

To better understand the functionality of the electrospun fibers in high humidity conditions and non-stable temperatures, water absorption of samples was studied as a function of time and temperature by considering the water contact angle (Water CAs), water uptake and the correlation between heat and mass transfer. Figure 8a shows the water contact angles of nonwoven fibrous mats of S1P2 to S5P2.

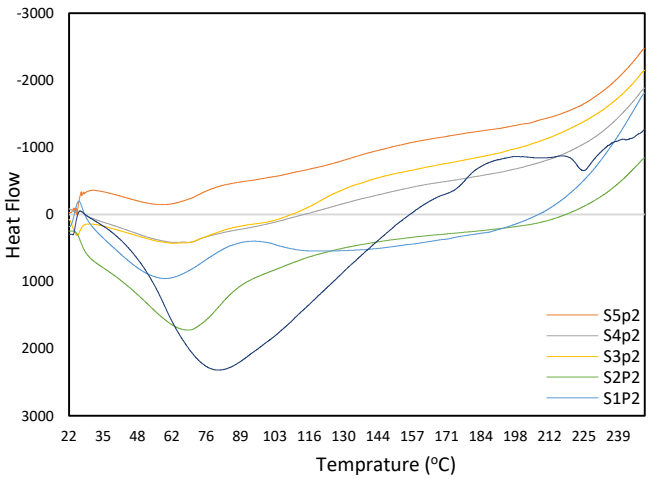

Figure 7 DSC thermograms of ASC and the electrospun fibers from collagen graft copolymers of different comonomer feed ratio, S1P2...S5P2; Aluminum Pans, heating rate of 10 °C.

Figure 5 ^{1}H NMR Spectra of the bulk collagen graft copolymers (A) and the electrospun fibers of collagen graft copolymers (B).

The water CA analysis indicates the high surface wettability of all samples. The water CAs decreased in the fiber samples from 80.33o to 56.21o in the first 10 seconds. The higher value of S1P2 is due to more hydrophilic end groups that can instantly make hydrogen bonding with the water droplet, by contrast to other fiber samples with higher branching densities that seem to penetrate into fiber samples as shown in decrease values of water CAs. After 10 minutes; as shown in Figure 8b, the water CA of S1P2 is still possessing a higher value of water CAs. This result is in a good agreement with the water absorption measured after 12 hours, Figure 8c; where the initial weight of bulk polymer S1P2 achieved a 43.64% growth in mass and fiber sample of S1P2 could gain only a weight increase of 24.03%. And also, a nonequivalent mass transfer was observed in fiber mass loss where the fiber samples were left to be dried at room temperature. This substantial deviation was not observed in other samples. Hence, it can be suggested that the increase in branching density can significantly reduce the destructive impact of electrospinning conditions on the ASC chains when it comes to the mass loss of the electrospun fibers in high humidity situations.

As shown in Figure 8d, the water absorption capacity of fiber samples was studied as a function of temperature where the fiber samples were soaked in water and were heated up to 100 ^{o}C for 9 h and then cooled down to room temperature (20 ^{o}C) for 11 hours. This measurement was accomplished to consider the impact of increased chain mobility on the absorption capacity of fibers as a consequence of increasing temperature on amphiphilic behavior of the samples having the flexible chains. It was observed that heating can accelerate the absorption behavior of the fiber samples in contrast with what is achieved at lower temperatures below the melting region, as specified in DSC, Figure 7.

It can be clearly observed that fiber samples of S1P2, S2P2, and S5P2 have shown a significant weight loss by increasing temperature above their melting point and have followed the same behavior in their cooling phase afterward. By contrast, the rest of the samples demonstrated a higher absorption behavior. Even though all samples lost their fibrous morphology after this test, S4P2 has shown a continuing absorption in the cooling stage. These observations are in agreement with increased chain flexibility as a result of increased temperature in the orientated chains up to melting region of each fiber sample. By contrast, above the melting region, when the side chains reach to their T_g. This heat transfer to the side chains can significantly preserve the main backbone chain that undergoes the degradation,

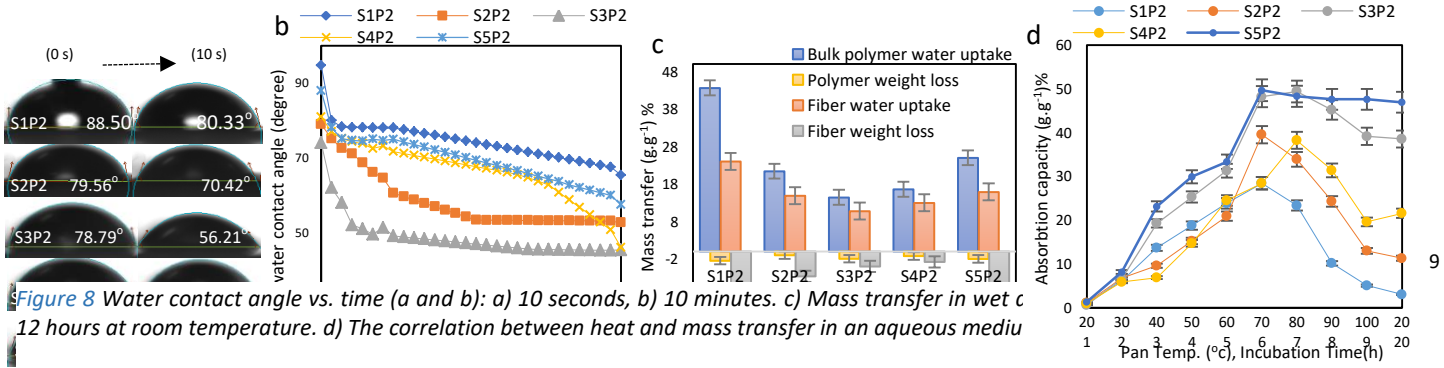

Figure 8 Water contact angle vs. time (a and b): a) 10 seconds, b) 10 minutes. c) Mass transfer in wet c 12 hours at room temperature. d) The correlation between heat and mass transfer in an aqueous mediu

otherwise. This can be clearly observed in the absorption capacity of S3P2, S4P3 after the cooling stage in which their weight loss is not significant.

CONCLUSIONS

In this study, Acid soluble collagen (ASC) was modified by a free radical copolymerization method using MMA-co-EA as applied comonomers. The density of branching was investigated by increasing monomer feed ratios in relation to grafting parameters, molecular weight of side branches, viscosity, surface tension and conductivity of the grafted copolymers. While some discussion was devoted to the synthesis, rheological and solid-state properties of the branched structure of collagen graft copolymers, this paper focused onto the influence of branching on fiber formation through electrospinning as a challenging processing method in relation to the delicate structure of acid soluble collagen. To avoid Rayleigh instability, the solution concentration was considered as a variable factor and the other parameters were kept approximately constant to consider the influence of branching on fiber characterizations. The surface characterizations were then performed on the processed collagen graft copolymers and compared with unprocessed collagen chains to study the effect of branching on physiochemical properties. The increased grafting performance is not the sole factor determining the processability of the grafted collagen copolymer. From surface characterizations, thermal stability and NMR analysis; the short chain branching of P(MMA-co-EA) can not only effectively influence the fiber morphology and the thermal stability of collagen graft copolymer, but also significantly reduce the degradation rate of the collagen chains during processing. By contrast, the long chain branching of ASC-g-P(MMA-co-EA) can provide a higher entanglement density, leading to the more uniformity of fibers. Hence, it can be concluded that a tailored side branching as a pretreatment can add unique properties and allow fiber formation from collagen chains that would otherwise be degraded during processing. This has a significant impact on new end-uses of collagen in a stable fibrous structure with enhanced properties.

REFERENCES

[1] I. Plesa, P.V. Notingher, S. Schlogl, C. Sumereder, M. Muhr, Properties of Polymer Composites Used in High-Voltage Applications, Polymers 8(5) (2016).

[2] M.S.M. Eldin, A.A. Elzatahry, K.M. El-Khatib, E.A. Hassan, M.M. El-Sabbah, M.A. Abu-Saied, Novel Grafted Nafion Membranes for Proton-Exchange Membrane Fuel Cell Applications, Journal of Applied Polymer Science 119(1) (2011) 120-133.

[3] Z. Bazrafshan, M. Ataeefard, F. Nourmohammadian, Modeling the effect of pigments and processing parameters in polymeric composite for printing ink application using the response surface methodology, Progress in Organic Coatings 82 (2015) 68-73.

[4] V. Pillay, A. Seedat, Y.E. Choonara, L.C. du Toit, P. Kumar, V.M.K. Ndesendo, A Review of Polymeric Refabrication Techniques to Modify Polymer Properties for Biomedical and Drug Delivery Applications, Aaps Pharmscitech 14(2) (2013) 692-711.

[5] Z. Bazrafshan, G.K. Stylios, Custom-built electrostatics and supplementary bonding in the design of reinforced Collagen-gP (methyl methacrylate-co-Ethyl Acrylate)/Nylon 66 core-shell fibers, Journal of the Mechanical Behavior of Biomedical Materials (2018).

[6] M. Curcio, U.G. Spizzirri, F. Iemma, F. Puoci, G. Cirillo, O.I. Parisi, N. Picci, Grafted thermo-responsive gelatin microspheres as delivery systems in triggered drug release, European Journal of Pharmaceutics and Biopharmaceutics 76(1) (2010) 48-55.

[7] C.F. Chi, Z.H. Cao, B. Wang, F.Y. Hu, Z.R. Li, B. Zhang, Antioxidant and Functional Properties of Collagen Hydrolysates from Spanish Mackerel Skin as Influenced by Average Molecular Weight, Molecules 19(8) (2014) 11211-11230.

[8] P.K. Binsi, B.A. Shamasundar, A.O. Dileep, F. Badii, N.K. Howell, Rheological and functional properties of gelatin from the skin of Bigeye snapper (Priacanthus hamrur) fish: Influence of gelatin on the gel-forming ability of fish mince, Food Hydrocolloids 23(1) (2009) 132-145.

[9] M.Y. Li, M.J. Mondrinos, M.R. Gandhi, F.K. Ko, A.S. Weiss, P.I. Lelkes, Electrospun protein fibers as matrices for tissue engineering, Biomaterials 26(30) (2005) 5999-6008.

[10] J.P. Chen, C.H. Su, Surface modification of electrospun PLLA nanofibers by plasma treatment and cationized gelatin immobilization for cartilage tissue engineering, Acta Biomaterialia 7(1) (2011) 234-243.

[11] T. Subbiah, G.S. Bhat, R.W. Tock, S. Pararneswaran, S.S. Ramkumar, Electrospinning of nanofibers, Journal of Applied Polymer Science 96(2) (2005) 557-569.

[12] P.R. Babu, T.P. Sastry, C. Rose, N.M. Rao, Hydrogels based on gelatin poly(hydroxyethyl methacrylate) and poly(butyl acrylate) graft copolymer impregnated with fibrin, Journal of Applied Polymer Science 65(3) (1997) 555-560.
[13] M. Sadeghi, H. Hosseinzadeh, SYNTHESIS AND PROPERTIES OF COLLAGEN-g-POLY(SODIUM ACRYLATE-co-2-HYDROXYETHYLACRYLATE) SUPERABSORBENT HYDROGELS, Brazilian Journal of Chemical Engineering 30(2) (2013) 379-389.
[14] A.K. Mohanty, M. Misra, G. Hinrichsen, Biofibres, biodegradable polymers and biocomposites: An overview, Macromolecular Materials and Engineering 276(3-4) (2000) 1-24.
[15] A. Bhattacharya, B.N. Misra, Grafting: a versatile means to modify polymers - Techniques, factors and applications, Progress in Polymer Science 29(8) (2004) 767-814.
[16] B.S. Kaith, R. Jindal, M. Maiti, Induction of Chemical and Moisture Resistance in Saccharum spontaneum L Fiber Through Graft Copolymerization with Methyl Methacrylate and Study of Morphological Changes, Journal of Applied Polymer Science 113(3) (2009) 1781-1791.
[17] H. Keles, M. Sacak, Graft copolymerization of methyl methacrylate onto gelatin using KMnO4-H2SO4 redox system, Journal of Applied Polymer Science 89(10) (2003) 2836-2844.
[18] Z.H. Sun, F.S. Chen, HOMOGENEOUS GRAFTING COPOLYMERIZATION OF METHYLMETHACRYLATE ONTO CELLULOSE USING AMMONIUM PERSULFATE, Cellulose Chemistry and Technology 48(3-4) (2014) 217-223.
[19] J. Bockova, L. Vojtova, R. Prikryl, J. Cechal, J. Jancar, Collagen-grafted ultra-high molecular weight polyethylene for biomedical applications, Chemical Papers 62(6) (2008) 580-588.
[20] B. Vazquez, M. Gurruchaga, I. Goni, HYDROGELS BASED ON GRAFT-COPOLYMERIZATION OF HEMA BMA MIXTURES ONTO SOLUBLE GELATIN - SWELLING BEHAVIOR, Polymer 36(11) (1995) 2311-2314.
[21] J.P. Zheng, S. Gao, J.X. Wang, K.D. Yao, Swelling behavior of gelatin-g-methyl methacrylate copolymers, Journal of Materials Science 40(15) (2005) 4029-4033.
[22] J.P. Zheng, J.X. Wang, S. Gao, K.D. Yao, Swelling behavior of gelatin-g-poly(butyl acrylate) copolymers, Journal of Applied Polymer Science 97(3) (2005) 1033-1037.
[23] J. Liu, L.Z. He, S. Ma, J.Y. Liang, Y. Zhao, H. Fong, Effects of chemical composition and post-spinning stretching process on the morphological, structural, and thermo-chemical properties of electrospun polyacrylonitrile copolymer precursor nanofibers, Polymer 61 (2015) 20-28.
[24] S.Y. Bak, G.J. Yoon, S.W. Lee, H.W. Kim, Effect of humidity and benign solvent composition on electrospinning of collagen nanofibrous sheets, Materials Letters 181 (2016) 136-139.
[25] D.I. Zeugolis, S.T. Khew, E.S.Y. Yew, A.K. Ekaputra, Y.W. Tong, L.Y.L. Yung, D.W. Hutmacher, C. Sheppard, M. Raghunath, Electro-spinning of pure collagen nano-fibres - Just an expensive way to make gelatin?, Biomaterials 29(15) (2008) 2293-2305.
[26] K. Hofman, N. Tucker, J. Stanger, M. Staiger, S. Marshall, B. Hall, Effects of the molecular format of collagen on characteristics of electrospun fibres, Journal of Materials Science 47(3) (2012) 1148-1155.
[27] G. Tronci, R.S. Kanuparti, M.T. Arafat, J. Yin, D.J. Wood, S.J. Russell, Wet-spinnability and crosslinked fibre properties of two collagen polypeptides with varied molecular weight, International Journal of Biological Macromolecules 81 (2015) 112-120.
[28] L. Yang, C.F.C. Fitie, K.O. van der Werf, M.L. Bennink, P.J. Dijkstra, J. Feijen, Mechanical properties of single electrospun collagen type I fibers, Biomaterials 29(8) (2008) 955-962.
[29] S. Heydarkhan-Hagvall, K. Schenke-Layland, A.P. Dhanasopon, F. Rofail, H. Smith, B.M. Wu, R. Shemin, R.E. Beygui, W.R. MacLellan, Three-dimensional electrospun ECM-based hybrid scaffolds for cardiovascular tissue engineering, Biomaterials 29(19) (2008) 2907-2914.
[30] S.A. Sell, M.J. McClure, K. Garg, P.S. Wolfe, G.L. Bowlin, Electrospinning of collagen/biopolymers for regenerative medicine and cardiovascular tissue engineering, Advanced Drug Delivery Reviews 61(12) (2009) 1007-1019.
[31] L. Buttafoco, N.G. Kolkman, P. Engbers-Buijtenhuijs, A.A. Poot, P.J. Dijkstra, I. Vermes, J. Feijen, Electrospinning of collagen and elastin for tissue engineering applications, Biomaterials 27(5) (2006) 724-734.
[32] N. Okutan, P. Terzi, F. Altay, Affecting parameters on electrospinning process and characterization of electrospun gelatin nanofibers, Food Hydrocolloids 39 (2014) 19-26.

[33] J.A. Matthews, G.E. Wnek, D.G. Simpson, G.L. Bowlin, Electrospinning of collagen nanofibers, Biomacromolecules 3(2) (2002) 232-238.
[34] C. Englert, T. Blunk, R. Muller, S.S. von Glasser, J. Baumer, J. Fierlbeck, I.M. Heid, M. Nerlich, J. Hammer, Bonding of articular cartilage using a combination of biochemical degradation and surface cross-linking, Arthritis Research & Therapy 9(3) (2007).
[35] H. Keles, M. Celik, M. Sacak, L. Aksu, Graft copolymerization of methyl methacrylate upon gelatin initiated by benzoyl peroxide in aqueous medium, Journal of Applied Polymer Science 74(6) (1999) 1547-1556.
[36] Z. Bazrafshan, G.K. Stylios, One-pot approach synthesizing and characterization of random copolymerization of ethyl acrylate-co-methyl methacrylate with broad range of glass transition temperature onto collagen, Polymer Engineering & Science 58(8) (2018) 1261-1267.
[37] X.F. Zheng, Q. Lian, H. Yang, H.X. Wu, C.H. Cheng, G.W. Yin, W.G. Zhang, Preparation and characterization of temperature-memory nanoparticles of MIP-CS-g-PMMA, Rsc Advances 6(112) (2016) 110722-110732.
[38] T. Kuwajima, H. Yoshida, K. Hayashi, GRAFT-POLYMERIZATION OF METHYL-METHACRYLATE ONTO GELATIN, Journal of Applied Polymer Science 20(4) (1976) 967-974.
[39] M. Hoshino, M. Takahashi, Y. Takai, J. Sim, Inhaled corticosteroids decrease subepithelial collagen deposition by modulation of the balance between matrix metalloproteinase-9 and tissue inhibitor of metalloproteinase-1 expression in asthma, Journal of Allergy and Clinical Immunology 104(2) (1999) 356-363.
[40] Q.H. Zhou, M. Bao, H.H. Yuan, S.F. Zhao, W. Dong, Y.Z. Zhang, Implication of stable jet length in electrospinning for collecting well-aligned ultrafine PLLA fibers, Polymer 54(25) (2013) 6867-6876.
[41] 3 - A brief description of textile fibers, Elsevier Ltd2016.
[42] S.A. Abbah, L.M. Delgado, A. Azeem, K. Fuller, N. Shologu, M. Keeney, M.J. Biggs, A. Pandit, D.I. Zeugolis, Harnessing Hierarchical Nano- and Micro-Fabrication Technologies for Musculoskeletal Tissue Engineering, Advanced Healthcare Materials 4(16) (2015) 2488-2499.
[43] N. Bhardwaj, S.C. Kundu, Electrospinning: A fascinating fiber fabrication technique, Biotechnology Advances 28(3) (2010) 325-347.
[44] R.T. Olsson, R. Kraemer, A. Lopez-Rubio, S. Torres-Giner, M.J. Ocio, J.M. Lagaron, Extraction of Microfibrils from Bacterial Cellulose Networks for Electrospinning of Anisotropic Biohybrid Fiber Yarns, Macromolecules 43(9) (2010) 4201-4209.
[45] M.G. McKee, G.L. Wilkes, R.H. Colby, T.E. Long, Correlations of solution rheology with electrospun fiber formation of linear and branched polyesters, Macromolecules 37(5) (2004) 1760-1767.
[46] E. Jeevithan, B. Bao, Y.S. Bu, Y. Zhou, Q.B. Zhao, W.H. Wu, Type II Collagen and Gelatin from Silvertip Shark (Carcharhinus albimarginatus) Cartilage: Isolation, Purification, Physicochemical and Antioxidant Properties, Marine Drugs 12(7) (2014) 3852-3873.
[47] Z.R. Li, B. Wang, C.F. Chi, Q.H. Zhang, Y.D. Gong, J.J. Tang, H.Y. Luo, G.F. Ding, Isolation and characterization of acid soluble collagens and pepsin soluble collagens from the skin and bone of Spanish mackerel (Scomberomorous niphonius), Food Hydrocolloids 31(1) (2013) 103-113.
[48] A. Pielesz, Temperature-dependent FTIR spectra of collagen and protective effect of partially hydrolysed fucoidan, Spectrochimica Acta Part a-Molecular and Biomolecular Spectroscopy 118 (2014) 287-293.
[49] S. Udhayakumar, K.G. Shankar, S. Sowndarya, S. Venkatesh, C. Muralidharan, C. Rose, L-Arginine intercedes bio-crosslinking of a collagen-chitosan 3D-hybrid scaffold for tissue engineering and regeneration: in silico, in vitro, and in vivo studies, Rsc Advances 7(40) (2017) 25070-25088.
[50] V. Singh, A.K. Sharma, D.N. Tripathi, R. Sanghi, Poly(methylmethacrylate) grafted chitosan: An efficient adsorbent for anionic azo dyes, Journal of Hazardous Materials 161(2-3) (2009) 955-966.

Highlights

- Grafting polymerization can be applied to modify the surface of acid soluble collagen before electrospinning.
- The side branches of the main backbone of collagen can significantly influence the initial viscosity of solutions to be electrospun.
- Increasing the number of branching onto ASC chains can significantly decrease the deteriorative impact of the electrospinning conditions.
- The grown branches onto the collagen chains can increase the stability of collagen-based fibers under high humidity conditions.
- The short chain branches onto collagen can influence the thermal stability of electrospun collagen fibers while the long chain branches can enhance the fiber uniformity due to the higher entanglement density.